



## Calculation of lateral velocity estimation and error discrimination for railway wheelset to avoid sliding

Zulfiqar Ali Soomro\*

\*Mechanical Engineering Department Quaid-e-Awam University of Engineering, Science and Technology  
Nawabshah, Pakistan

---

**Article info:**

Received: 01/02/2017

Accepted: 27/11/2018

Online: 27/11/2018

**Keywords:**

Creep force,

Creepage,

Creep coefficient,

Adhesion,

Solid axle.

**Abstract**

Lateral velocity has very backbone position in the railway vehicle wheelset dynamics as it usually becomes the cause of derailment by sliding due to insufficient adhesion ratio. This inappropriate balance is pretext owing to contamination and weather procures the disturbances. This perturbation makes hindrances in the proper running of wheelset on track. To analyze the noise, the Kalman filter is used based upon the railway dynamic modeling to estimate the actual signals to control the noise by measurement. Thus error percentage is also computed to detect the slippage by adhesion on applicable analysis of creep coefficient. Since controllable estimated lateral velocity assures minimum wheel slide.

---

**1. Introduction**

The conservative rail vehicles comprise of two conical wheelsets fastened upon regular axle premise lateral motions from small noise on its rolling. When the speed of rolling is slow, then the lateral movements congregate to zero at tracking center position. But, at a certain higher speed, the railway wheels diminish its stability and declare its instability of motion stated by Uzzal et al. [1] and Zeng and Wu [2].

The lateral speed of railway wheels is the constituent of the vehicle speed vector vertical to the vehicle direction, similar to the floor plane. No acceptable way is available to measure the lateral speed on fabrication railway vehicles

and its wheels. This observes the estimation of lateral speed using state observers as a sensible solution for detection of noise. The estimations of the lateral velocity of a railway vehicle are helpful to improve vehicle system control and wheels for the steering system to reduce disturbance as described by Aalami et al. [3].

In the rolling theory of rail-wheel, the peripheral creep forces have a very important function. The researcher contravened 2D dilemma for rail wheel get in touch with undulating through locomotive wheelset and railroad. He sustained that the lateral creep forces should not surpass the Coulombs utmost boundary. Model of Carter only measured the association between the longitudinal creepage and the tangent forces on

---

Corresponding author

email address: zulfiqarali\_s@yahoo.com

the patch area in the researches of Kim [4] and Li et al. [5].

The dynamics of lateral velocity of railway vehicle wheelset system is stalwartly predisposed by the contacting forces and concerned moments occurring in the rail wheel interacting regions resembling nearly elliptical in shape. When the rail wheel is disturbed from the middle location on a tangential track, bulky straight acting forces produced at the rail-wheel touch are known as creeping forces. These affecting horizontal forces are accountable for hunting of Bogie in railway transport stated by Grip et al. [6].

One influential issue like Derailment is apprehensive with those occurring in lateral vehicle oscillations causing wheels to mount over the railway head or rail tracks. Railway dynamic factors like rolling radius difference, wheel contact angles, interface areas, rolling radius difference and elliptical forms are nonlinear functions for lateral budge of the railway wheelset pertaining to the track centerline of rail tracks as mentioned by Ahmadi et al. [7]. Hence the railway car body will have less sway on the bogie of a railway vehicle and rail wheels are concerned to lateral velocity in railway dynamics. Therefore, the bogie of single railway vehicle and wheels are well thought-out for assessing the lateral velocity dynamics. On the other hand, the weight of the railway car body is used into description on scheming of the Kalker’s coefficients for dynamics explained by Li and Cheng [8].

Through the traditional Kalman filter (KF) study, the modeling of estimation dilemma gains crucial information for the processing and measuring the perturbed data studied by Wenzel et al. [9] and Ward et al. [10]. In several realistic conditions, the pertaining data are conceived sick identified. In almost favorable estimate outcomes, accurate information of the processing disturbance and measuring of the perturbed data is requisite, though, these are typically indefinite in observation. Hence a Kalman estimator with incorrect preferable figures may guide to large filtration errors and yet to a discrepancy of errors in the running system further worked by Hussain et al. [11] and Mei et al. [12].

The monitoring of lateral vehicle motion can be conceived by using accurate monitoring models and reliable estimation algorithms [13]. They used Bucy Kalman filter in their investigation.

In this paper, the contact mechanics is used for modeling railway wheelset, described in Section 2, and Kalman filter scheme is used and error discrimination is defined in Section 3 and 4, respectively; finally, the results are simulated in Section 4.

## 2. Contact mechanics for rail-wheel modeling

The lateral oscillations for the railway wheels monitored through creeping forces are produced at the wheel-rail interface as studied by Hussain, et al. [14]. The rail-wheel interfacing forces can be torn into usual and lateral forces at the rail wheel contacts studied by Soomro et al. [15]. The lateral forces at wheelset can be led using longitudinal ( $X_w$ ) and lateral ( $Y_w$ ) motions (Eqs. (1 and 2), respectively) along with torsional motion ( $O_w$ ) generated by the solid axle with respect to the center line of railway track [15].

$$v_{wL} = \omega_{wL} \cdot [r_o + \gamma(y_L - w)] \tag{1}$$

This is left wheel velocity as described in Eq. (1)

$$v_{wR} = \omega_{wR} \cdot [r_o - \gamma(y_R - w)] \tag{2}$$

Above is right wheel velocity

Lateral creepage of the left and right wheels w.r.t spin are:

$$F_{yR} = f_{22} \lambda_{yR} \tag{3}$$

$$F_{yL} = f_{22} \lambda_{yL} \tag{4}$$

where lateral creep force for the wheels by ‘ $f_{22}$ ’ is known as creep coefficient.

Thus lateral force for right wheel is linearized as under

$$F_{yR} = N_R \frac{\lambda_{xR} + \lambda_{yR}}{\lambda^2_R} \left[ \frac{\partial \mu_R}{\partial \lambda_R} - \frac{\mu_R}{\lambda_R} \right]_{(\lambda_{xR}, \lambda_{yR})} \times \Delta_{\lambda_{xR}} + N_R \left[ \frac{\lambda^2_{yR}}{\lambda_R} \frac{\partial \mu_R}{\partial \lambda_R} + \frac{\lambda^2_{xR}}{\lambda^2_R} \frac{\mu_R}{\lambda_R} \right]_{(\lambda_{xR}, \lambda_{yR})} \times \Delta_{\lambda_{yR}} \tag{5}$$

Thus the right wheel is represented by small signal model by sensors.

$$\Delta F_{yR} = g_{21}\Delta\lambda_{xR} + g_{22}\Delta\lambda_{yR} \quad (6)$$

Similarly, the lateral force for the left wheel is linearized and converted by small signal model for Kalman filter [15].

$$\Delta F_{yL} = g_{21}\Delta\lambda_{xL} + g_{22}\Delta\lambda_{yL} \quad (7)$$

### 3. Kalman filter design scheme

After framing above small signal model converted from above dynamic equations, a Kalman filter is invented to filter the zones of the railway model at precise contact on the creeping curves. The tangential speed dynamics for the wheelset are animated by anonymous path noise formulated by Kalman estimators which are more comprehensive. This difficulty can be resolved by inserting the unknown parameter into the state equation as the state vector quite as an input so that dynamical system remains unaffected as described by Wenzle et al. [9]. The state and measurement terms for a nonlinear system, are enumerated as:

$$y_{lat(o/p)} = H(x) + v \quad (8)$$

where,  $\dot{x}$  is state of the system by vector;  $y$  is measuring system vector while  $w$  and  $v$  are processing and measuring disturbances, correspondingly. The distinct-time based lateral speed dynamical system is explained in the KF phenomenon by the following vector distinction mathematical equations:

$$x_{k+1} = \Phi x_k + w_k \quad (9)$$

$$y_k = Hx_k + v_k \quad (10)$$

The averaged and covariance factor of the preliminary state are described as:

$$\hat{z}(0|0) = \hat{z}_0, \hat{S}(0|0) = Z_0 \quad (11)$$

In accumulation to this, the primary average and the covariance of the disturbances are explained as:

$$\hat{q}_0 = q_0, \hat{Q}_0 = Q_0, \hat{r}_0 = r_0, \hat{R}_0 = R_0 \quad (12)$$

Here  $q_k$  and  $Q_k$  are the average and covariance for process disturbance in that order;  $r_k$  and  $R_k$  are also the average and covariance for measuring the disturbances, correspondingly. The proposed Kalman estimator/filter calculation is thus classified by three portions, time update, measurement update, and noise estimation.

### 4. Error value discrimination

Estimation result proves that the correctly infused Kalman filter can offer a consistent estimation for wheelset positions at the exact working condition. The filtered tangential motion with guessed error is often superior to predictable spin values with estimation error. The tangential Motion is directly exaggerated by path noise hence its inference is better than that of the spin angle [14].

$$Error\% = \frac{|z_{estimate} - z_{measurement}|}{\max(|z_{measurement}|)} \times 100$$

Here the actual error curve is assumed for estimation standards, and the usual error [12] specified by  $Z_{measurement}$  is the output value of railway model, and  $Z_{estimate}$  is the filtration parameter, whereas the errors are the values among the estimation and the output parameters as described in Kalman filter Section.

### 5. Results and discussion

Let us consider a wheelset deflected laterally from a pure rolling position by a distance  $y$ , as the initial state, while on a straight track, the pure rolling position is the centerline of the track. On rolling forward with a velocity  $v$ , the deflected wheelset wants to roll to the preferred state. If the wheelset is constrained to remain in a similar attitude to the track, as it is in the initial state, creepage/slip takes place as the wheels roll [16, 17, 18]. In the case illustrated, the wheel of

larger rolling diameter slips back, and the smaller rolling diameter wheel slips forward. Longitudinal creepage is defined as the ratio of the creep velocity to the forward velocity of the wheelset. Slip force,  $F_s$  is generated on the wheelset which reacts against the constraining force at the journal. The force opposite to  $F_s$  is acting on the rail. The amount of creepage and the creep force generated are directly proportional to the displacement  $y$  and the cone angle  $\gamma$ .

The lateral dynamics in terms of velocity of the railway vehicle is described as follows by verifying the three different varieties of creep coefficients to watch its behavior by utilizing Kalman filter. Thus error percentage value is based upon estimation to avoid derailment by slip and sliding.

5.1. Lateral velocity of wheelset at different creep coefficients

The lateral velocity of a railway wheelset on the railway track is shown in the Figs. 1 to 4; where the lateral motion of the railway wheelset is testified by three different coefficients of the creep versions to watch the performance of the railway wheelset. The head every head of curve ends by estimated parameter.

In Fig. 1, when coefficient of the creep is taken as  $6e+7$  as the higher value, it is observed that the lateral velocity of the railway wheelset moves with motion slightly above 0.02 meter/s initially to 0.03 m/s under 0.5 seconds in chaos zigzag manner with time intervals from 0.5 to 5 s consisting upon actual and estimated parameters. Here the actual values denoted by blue color moves along with the estimated values which are denoted by red color in peaks. The peaks are nearly touching the bordering plane slightly above the -0.01 m/s in 5 s majorly with the estimated parameter. Every head of the curve ends by the estimated parameter.

In the Fig. 2, when the coefficient of the creep is proposed as  $1e+6$ , the lateral velocity of the railway wheelset varies for the estimated parameters from slightly lower than 0.04 m/s to above 0.1m/s in a curved way in 1 s. Then it diverts into horizontal way with smaller perturbations from 0.1 m/s to along with 0.13

m/s in 5 s. Whereas the actual signal with the smaller disturbances starts from slightly above 0.02 m/s in the zone of 0.02 m/s to end at -0.02 m/s in 5 s by disordered zigzag manner through touching its up and down borders. Here both actual and estimated values vary and run at some distance from each other.

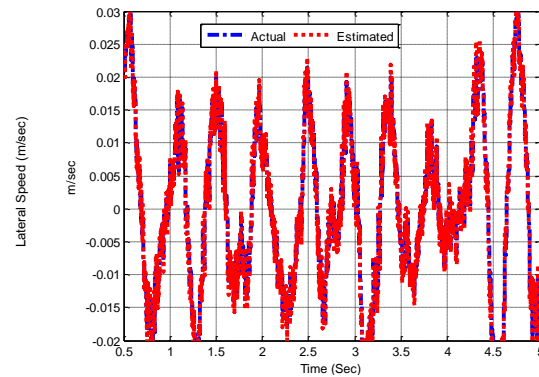


Fig. 1. Lateral velocity of wheelset at  $f_{11} = 1e+7$  creep coefficient.

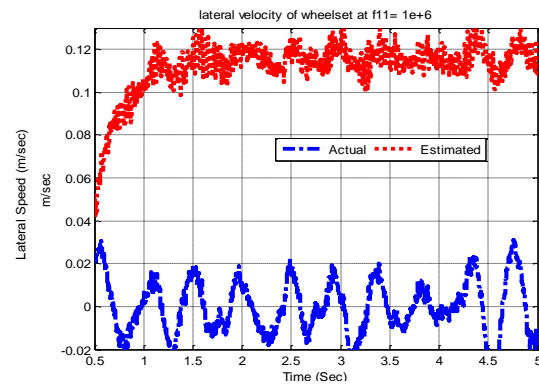
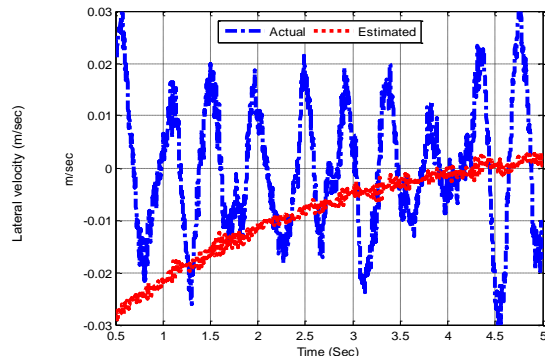


Fig. 2. Lateral velocity of wheelset at  $f_{11} = 1e+6$  creep coefficient.

In Fig. 3, when the coefficient of the creep is proposed as  $1e+5$  then the lateral velocity of the railway wheelset varies from lower than -0.03 m/s to above 0 m/s for the estimated parameter upward with smaller perturbations in curved shape 5 s. Whereas the actual signal, with the smaller disturbances, starts from slightly above -0.02 m/s to 0.03 m/s to end in 5 s by the unarranged zigzag way. Here the estimated values overlap the actual parameter in a time period of 5 s.

This shows that when the creep coefficient is higher, then both actual and estimated parameters overlap each other, but whenever the

coefficient of the creep decreases then both the actual and estimated values curves are separated from each other by significant difference at the smaller distance except here in 3<sup>rd</sup> case.



**Fig. 3.** Lateral velocity of wheelset at  $f_{11} = 1e+5$  creep coefficient.

5.2 Error estimation for lateral velocity of wheelset

The rail wheel track dynamic parameters are estimated to analyze the error ratio through high creep coefficient by a black line and low creep coefficient by a blue line. The higher coefficient of creep is selected as  $1e+7$  and the lower coefficient is taken as  $1e+6$  for estimation of error. The mentioned high and low creep coefficient values are applied to estimate the error ratio for the lateral velocity of a wheelset of the train shown in Fig. 4. Here the black line represents high creep coefficient travels in a straight direction with small noise from zero error measured scale. This means that there is no error in adhesion to occur slip shows increasing creep. While low creep coefficient denoted by the blue line passes through -0.04 to 6.5 percentage in vertical scale of error value in a zigzag way with major disturbances, then it travels downwardly below zero in 0.3 s to end on -0.1 in one second showing improper sufficiency of adhesion. Such condition shows the slip and sliding of the wheelset.

In Fig. 4, a higher value for error estimation is denoted by e1 by creep coefficient and e2 is displayed by lower error estimation depending upon the coefficient of the creep with time in second with the horizontal direction.

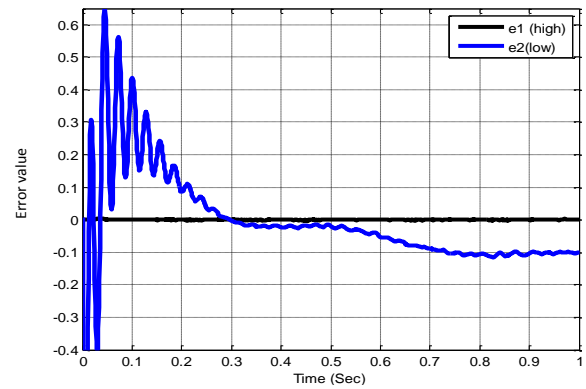


**Fig. 4.** Error estimation for lateral velocity of wheelset.

6. Conclusions

In this paper, simple dynamics pertaining to the lateral velocity is enumerated to frame a railway model. Mathematical model formulations are then manipulated for the usage of Kalman filter. Three different values of creep coefficients are devised by Kalman filter strategy for estimating the occurring noise with an actual parameter to stabilize the system. Then the error percentage is established to detect the adhesion to control slip based upon creep coefficient application. It is assumed that when a high creep coefficient is utilized then both the actual and estimated travel parallel overlap each other in a zigzag manner. But when the creep coefficient decreases then the both are separated from each other with small noise and zigzag way. The attitude of the estimated curve shows little but higher adhesion along with creepage denoting slip reduction.

The error estimation shows no slip on higher creep coefficient on constant adhesion, but in decreasing creep coefficient, the curve shows unbalancing in curve suggesting a decrease in adhesion and creep leading to being constant.

References

[1] R. U. A. Uzzal, W. Ahmed, and S. Rakheja, "Dynamic analysis of railway vehicle-truck interactions due to wheel flat with a pitch-plane vehicle model", *Journal of Mechanical Engineering*, Vol. ME39, No. 2, pp. 12-02, (2008).

- [2] J. Zeng, and P. Wu, "Study on the wheel-rail interaction and derailment safety", *Wear*, Vol. 265, pp. 1452-1459, (2008).
- [3] M. R. Aalami, A. Anari, T. Shafighfard, and S. Talatahari, "A Robust Finite Element Analysis of the Rail-Wheel Rolling Contact", *Advances in Mechanical Engineering*, Vol. 2013, Article ID 272350, (2013).
- [4] J. Kim, "Effect of vehicle model on the estimation of lateral vehicle dynamics," *Int. J. Automot. Technol.*, Vol. 11, No. 3, pp. 331-337, (2010).
- [5] L. Li, J. Song, L. Kong, and Q. Huang, "Vehicle velocity estimation for real-time dynamic stability control," *Int. J. Automot. Technol.*, Vol. 10, No. 6, pp. 675-685, (2009).
- [6] H. F. Grip, L. Imsland, T. A. Johansen, J. C. Kalkkuhl, and A. Suissa, "Vehicle sideslip estimation: Design, implementation and experimental validation," *IEEE Control Syst. Mag.*, Vol. 29, No. 5, pp. 36-52, (2009).
- [7] J. Ahmadi, A. K. Sedigh, and M. Kabganian, "Adaptive vehicle lateral plane motion control using optimal tire friction forces with saturation limits consideration," *IEEE Trans. Veh. Technol.*, Vol. 58, No. 8, pp. 4098-4107, (2009).
- [8] S. H. Lee, and Y.C. Cheng, "A New Dynamic Model of High Speed Railway Vehicle Moving on Curved Tracks," *Journal of Vibration and Acoustics*, Vol. 130, 2008.
- [9] T. A. Wenzel, K. J. Burnham, M. V. Blundell et al. "Dual extended Kalman filter for vehicle state and parameter estimation" *Journal of Vehicle System Dynamics*, Vol. 44, No. 2, 1532171, (2006).
- [10] C. Ward, E. Stewart, H. Li, R. Goodall, C. Roberts, T.X. Mei, G. Charles and R. Dixon, "Condition monitoring opportunities using vehicle based sensors". *IMECHE Proceedings, Part F: Rail and Rapid Transit*, Vol. 225, No. 2. pp. 202-218, (2011).
- [11] I. Hussain, T. X. Mei, A. A. H. J. "Modeling and Estimation of Nonlinear Wheel-rail Contact Mechanics". *Proceedings of the twentieth International conference on System Engineering*, pp. 219-223, (2009).
- [12] T. X. Mei, Hussain, "Multi Kalman filtering approach for estimation of wheel-rail contact conditions". *Proceedings of the United Kingdom Automatic Control Conference, Coventry, UK*, pp. 459-464, (2010).
- [13] Sangoh Han, Kunsoo Huh, "Monitoring System Design for Lateral Vehicle Motion", *Vehicular Technology IEEE Transactions on*, Vol. 60, pp. 1394-1403, (2011).
- [14] I. Hussain, T. X. Mei, and M. Mirzapour, "Real Time Estimation of the Wheel-Rail Contact Conditions Using Multi-Kalman Filtering and Fuzzy Logic". In: *Control (Control), 2012 Ukacc International Conference On*, 3-5 Sept., pp. 691-696, (2010).
- [15] ZA Soomro, I. Hussain, B. S. Chowdhary, "Modeling and analysis of linearized wheel- rail contact dynamics". *Mehran University Research Journal of Engineering & Technology*, Volume 33, No. 3, pp. 335-340, (2014).
- [16] ZA. Soomro, "Step response and estimation of lateral and yaw motion disturbance of rail wheelset". *Journal of Engineering and Technology*, Vol. 5, No. 1, pp. 8-13, (2015).
- [17] ZA Soomro, "Dynamical attitude of non-linearly parameters of rail wheel contact on application of creep coefficient". *NUST Journal of Engineering Sciences*, Vol. 9, No. 1, pp. 13-17, (2016).
- [18] ZA Soomro, "Parametric dynamics of railway vehicle-track interaction model: The influence of creep coefficients" *J. Coupled Syst. Multiscale Dyn.*, Vol. 5, No. 1, pp. 33-37, (2017).

**How to cite this paper:**

Zulfiqar Ali Soomro, "Calculation of lateral velocity estimation and error discrimination for railway wheelset to avoid sliding" *Journal of Computational and Applied Research in Mechanical Engineering*, Vol. 8, No. 2, pp. 145-151, (2019).

**DOI:** 10.22061/jcarme.2018.2274.1212

**URL:** [http://jcarme.sru.ac.ir/?\\_action=showPDF&article=949](http://jcarme.sru.ac.ir/?_action=showPDF&article=949)

